Coexistence of magnetism and ferroelectricity in perovskites

Alessio Filippetti and Nicola A. Hill
Materials Department, University of California, Santa Barbara, California 93106-5050
(Received 18 December 2000; revised manuscript received 25 October 2001; published 7 May 2002)

We present a first-principles comparison of $BaTiO_3$, $CaMnO_3$, and $YMnO_3$ which reveals the fundamental role of the *d* electron occupation in preventing or favoring the simultaneous presence of magnetic and electric polarization. The ferroelectric compounds are distinguished from the nonferroelectrics by an ultrasensitivity of the *p*-*d* charge hybridization to the atomic displacements. To be effective these hybridization changes require the *d* orbitals oriented in the direction of the ferroelectric distortion to be formally empty. This orbital directionality can explain the coexistence of antiferromagnetism and ferroelectricity in the hexagonal phase of $YMnO_3$, which is ferroelectric along the *c* axis: in the Mn^{3+} ion, four filled *d* orbitals provide a magnetic moment, and one empty *d* orbital (d_z^2) can participate in hybridization changes and induce a ferroelectric distortion. The Born effective charges are found to be highly anomalous in $CaMnO_3$, which is far from being ferroelectric.

DOI: 10.1103/PhysRevB.65.195120 PACS number(s): 71.20.−b, 75.50.Ee, 77.80.−e, 77.84.Bw

I. INTRODUCTION

Perovskite materials are fascinating both because they display a wide variety of fundamental properties, from magnetism to ferroelectricity, from colossal magnetoresistance to half-metallicity, and because they are used in a number of important technological applications, such as transducers and memories. They also show electronic and structural peculiarities including orbital and charge ordering, formation of local moments, and Jahn-Teller distortions. Such a richness, combined with their relatively simple structure, makes them ideal materials for investigating the general principles that govern these properties.

For example in the recent past an understanding of the fundamentals of ferroelectricity has been gained by density functional theory studies of the perovskite ferroelectrics (e.g., $BaTiO_3$, $SrTiO_3$, and $KNbO_3$).[1,2] These studies have benefited from important theoretical advances such as linear-response density functional theory[3] and the Berry phase approach,[4,5] which allowed the formulation of the so-called modern theory of polarization in crystals. In addition, the ability to calculate dielectric permittivity, piezoelectricity, Born effective charge (BEC), pyroelectricity, and spontaneous electrical polarization (**P**) from first principles has led to important insights.

In parallel with (but apparently without intersecting) the current of studies on ferroelectric perovskites, a large community, driven by the discovery of colossal magnetoresistivity in Ca-doped $LaMnO_3$,[6] has started to investigate the vast class of magnetic (especially manganese) perovskites. Many magnetic perovskite oxides are antiferromagnetic insulators, but the possible magnetic phases (i.e., the ordering of magnetic moments) are diverse and dependent on the specific compound.

The lack of overlap between researchers studying magnetic perovskites and those studying ferroelectric perovskites is due to the fact that the cubic (or orthorhombically distorted) magnetic perovskites are generally not ferroelectric, whereas ferroelectricity is a common characteristic of the cubic perovskites having cations with zero *d* occupations (e.g., Ti^{4+}, Nb^{5+}).[7] However, the "d^0-ness" criterion for ferroelectricity does not rule out completely the simultaneous presence of magnetic and ferroelectric ordering. Indeed, the less widely studied class of *hexagonal* perovskites (to which $YMnO_3$ belongs) has been known for a long time to display both these properties. Understanding how the chemical environment affects the coexistence of magnetism and ferroelectricity is the main goal of this paper.

The primary focus of our investigation is the distribution of the electron charge within the *d* orbitals of both magnetic and ferroelectric perovskites. Indeed, many properties of these materials are crucially dependent on the *d*-orbital occupation numbers. They may display unusual features such as charge and orbital ordering, which, in turn, determine the magnetic ordering. Even the structural properties can be closely related to the *d*-state occupations. For example, the ions Mn^{3+} and Cr^{2+} belong to the class of Jahn-Teller compounds, in which the fractional occupation of the degenerate e_g orbitals drives the structure to an orthorhombic distortion, whereas the Mn^{4+} and Cr^{3+} ions, with their spherical t_{2g}^3 configuration, are chronically octahedral.

Also, the *d*-orbital occupation is a fundamental parameter in understanding the presence or absence of ferroelectricity. Past works have clearly shown that hybridization of cation *d* and anion *p* states is necessary to have a ferroelectric ground state,[1,2] whereas a ferroelectric state is never stable in primarily ionic compounds. Furthermore, previous work on ferroelectric perovskites[8–12] has clearly shown that the BEC tends to be anomalously large, i.e., far larger than the nominal ionic charges, in ferroelectric materials. The anomaly is believed to be a necessary condition for a crystal to sustain spontaneous **P**, since it indicates that **P** is very sensitive to (or may be driven by) small changes of atomic positions.

However, neither strong *p*-*d* hybridization nor anomalous BEC can be considered sufficient conditions for ferroelectricity. Indeed, hybridization is present in many nonferroelectric systems as well;[13] thus, it is not a very selective requirement, and the BEC are found to be anomalous even in nonferroelectric compounds.[14–16] We will show in this paper

that the driving force towards the ferroelectric state is in fact the sensitivity of the charge hybridization to ferroelectric displacements.[8] In this picture, the off-center displacements are energetically favored only if they are accompanied by a substantial rearrangement of the charge producing a charge imbalance between cation-anion bonds. This imbalance leads naturally to a destabilization of the centrosymmetric configuration.

In order to quantify this effect, a comparative study of the BEC, orbital occupations, ionic charges, and charge hybridizations in ferroelectric and nonferroelectric perovskites is required. We expect to see important differences of hybridization changes for ferroelectric and nonferroelectric materials. It will be shown that such differences do exist and are perhaps better indicators of the onset of ferroelectricity than an anomalous BEC alone.

Specifically, we present first-principles results for cubic $BaTiO_3$, cubic $CaMnO_3$, and hexagonal $YMnO_3$. $BaTiO_3$ is a well-studied ferroelectric (and nonmagnetic) perovskite. Our calculations for this compound are not aimed at elucidating new physics, but rather provide a reference point with which to compare the two other systems. In particular, $CaMnO_3$ shares the same nominal ionic configuration as $BaTiO_3$, although $CaMnO_3$ is magnetic and not ferroelectric. Finally, hexagonal $YMnO_3$ is probably the best known material in which both ferroelectric and magnetic orders coexist, and thus is the main focus of this work. The importance of *d*-state occupations is particularly evident here. Indeed, $YMnO_3$ can be grown in both cubic and hexagonal phases (although the latter is the most stable) but, despite the presence of the same Mn^{3+} ion, only the hexagonal structure is ferroelectric. This indicates that the possibility of coexistence does not depend just on the total amount of *d* charge, but, crucially, on the specific charge distribution within the *d* orbitals and their hybridizations with the surrounding environment.

The remainder of this paper is organized as follows: in Sec. II we describe our methodology and review the basic relationships between **P**, BEC, and orbital occupation numbers. In Secs. III A, III B, and III C we describe our results for $BaTiO_3$, $CaMnO_3$, and $YMnO_3$, respectively. Our conclusions are summarized in Sec. IV.

II. DEFINITIONS AND TECHNICAL DETAILS

In this work we use a plane-wave pseudopotential implementation[17] of density functional theory within the local spin density approximation[18] (LSDA). We use efficient ultrasoft[19] pseudopotentials which allow us to obtain accurate results at very feasible cutoff energies (30 Ry for $BaTiO_3$ and $CaMnO_3$, 35 Ry for $YMnO_3$). For Y, Ba, and Ti the semicore *s* and *p* electrons are treated as valence charge. In order to have highly transferable pseudopotentials, two projectors per angular channel are included in all the atoms. For total energy calculations we use up to $8\times8\times8$ grids of special k points.[20] Structural relaxations are performed by minimization of the Hellman-Feynman forces within a convergency threshold of 10^{-3} Ry/bohr.

Since many of the conclusions in this paper are reached from a density of states (DOS) analysis, we take care to calculate the DOS very accurately: the energies of a large (order 100) *k*-point set are interpolated using the linear tetrahedron method through the irreducible Brillouin zone. In order to calculate the DOS contributions coming from individual orbitals, we calculate the orbital occupation numbers $q_{j,lm\sigma}$ as the projections of Bloch states $\psi_{n\mathbf{k}\sigma}$ onto atomic wave functions $\phi_{j,lm}$:

$$q_{j,lm\sigma}=\sum_{\substack{n\mathbf{k}\\ occ}} \langle\psi_{n\mathbf{k}\sigma}|\phi_{j,lm}\rangle\langle\phi_{j,lm}|\psi_{n\mathbf{k}\sigma}\rangle, \tag{1}$$

where *j* runs over the atoms, and *lm* and σ are orbital and spin quantum numbers, respectively.

Much of the literature on first-principles studies of ferroelectrics focuses on the BEC as an indicator of the tendency to undergo ferroelectric distortion. The BEC ($Z^*_{j,\alpha\beta}$) is the atomic position derivative of **P** (at zero macroscopic electric field):

$$Z^*_{j,\alpha\beta}=\frac{\delta P_\alpha}{\delta R_{j,\beta}}, \tag{2}$$

where α and β are Cartesian indices. Alternatively, the BEC can be defined as the linear-order coefficient between the electric field $\mathcal{E}$ and the force $\mathbf{F}_j$ which the field exerts on ion *j*:

$$Z^*_{j,\alpha\beta}=\frac{\delta F_{j,\alpha}}{\delta \mathcal{E}_\beta}, \tag{3}$$

where the derivative is calculated at zero atomic displacement. A large BEC indicates that the force acting on a given ion due to the electric field generated by the atomic displacements is large even if the field is small, thus favoring the tendency towards a polarized ground state.

A number of different approaches for calculating the BEC have been presented in the literature based, in rough chronological order, on empirical methods,[21] supercell calculations,[22] linear-response density functional theory,[3] and Berry phase formulation.[4,5,23] Here we adopt a supercell approach based on the definition of Z^*_j given in Eq. (3) that has been shown to give accurate results.[22] Using the Hellmann-Feynman theorem, the force due to an external (i.e., bare) electric field $\mathcal{E}^{ex}$ (at zero displacement) is

$$F_{j,\alpha}=-Z_j|\mathcal{E}^{ex}_\alpha|+\sum_{n\mathbf{k}}\left\langle\psi_{n\mathbf{k}}\left|\frac{\partial V^{pp}}{\partial \mathbf{R}_j}\right|\psi_{n\mathbf{k}}\right\rangle. \tag{4}$$

The first term on the right-hand side of Eq. (4) is the force acting on the ion-core charge Z_j. The second term is the force due to the *response* of the electron density to the external perturbation. (V^{pp} is the ionic pseudopotential, and $\psi_{n\mathbf{k}}$ are the Bloch eigenfunctions of the perturbed system). From Eq. (4) the electric field derivative of $F_{j,\alpha}$ can be evaluated by finite differences.

The disadvantage of this approach is the necessity of using supercells: the bare electric field $\mathcal{E}^{ex}$ is simulated by a sawlike potential, and in order to make the atoms insensitive to this artifact, long supercells in the direction of the applied

field are needed (see Ref. 22 for details). On the other hand, its appeal resides in the fact that it does not require code implementations beyond ordinary total energy and forces calculations. For our cubic perovskites we use slabs with the axis parallel to **P**, respectively 4 times longer than those of the corresponding primitive cells (giving 20 atom slabs).

Within this method the optical dielectric tensor $\epsilon^{\infty}_{\gamma\beta}$ can be extracted as the ratio between the external and the total electric field into the slab. The longitudinal effective charges (LEC) $Z^{L}_{j,\alpha\beta}$ can be calculated as well. Like the BEC, the LEC's are defined through Eqs. (2) and (3), but with $\mathcal{E}$ replaced by $\mathcal{E}^{ex}$:

$$Z^{L}_{j,\alpha\beta}=\frac{\delta F_{j,\alpha}}{\delta \mathcal{E}^{ex}_{\beta}}=\sum_{\gamma} Z^{*}_{j,\alpha\gamma}\frac{1}{\epsilon^{\infty}_{\gamma\beta}}. \tag{5}$$

III. RESULTS

A. $BaTiO_3$

The purpose of this section is to provide benchmark calculations for this prototypical perovskite ferroelectric with which to compare our later calculations on magnetic ferroelectric and nonferroelectric perovskites. $BaTiO_3$ has been studied intensively in the past since the discovery of its ferroelectricity.[24] It shows a very rich phase diagram: in the high-temperature paraelectric phase it is a cubic insulator but, as the temperature is lowered, it undergoes three consecutive ferroelectric distortions along directions [001] (tetragonal), [110] (orthorhombic), and [111] (rhombohedral) at $T\sim 400$ K, 280 K, and 185 K, respectively. (A hexagonal ferroelectric phase has been observed[25] as well.) Many first-principles studies have been carried out,[1,2,26–29] and the structural and electronic properties, BEC's, spontaneous **P**, interatomic force constants, and phonon frequencies have been calculated.

Here we are specifically interested in studying the DOS, orbital hybridization, and occupation numbers. Although a number of DOS calculations for $BaTiO_3$ have already been carried out (see, for instance, Ref. 2), our revisitation is necessary since we want to evaluate the individual contribution to the total DOS of anion *p*, and cation *d* e_g, and t_{2g} orbitals. This orbital resolution (to our knowledge never reported so far) is crucial for our later comparison with the DOS of the magnetic perovskites.

In Fig. 1 (upper panel) our DOS calculation for the cubic phase of $BaTiO_3$ is shown. The DOS is resolved into O *p* and Ti *d* contributions. The latter is further resolved into parts coming from the t_{2g} triplet and the e_g doublet of orbitals. The DOS is that of a charge-transfer insulator, with the valence-band top almost purely O *p* type and the conduction-band bottom completely Ti *d* type.

$BaTiO_3$ is usually described as a rather ionic material with a nominal $Ba^{2+}Ti^{4+}O_3{}^{2-}$ configuration, but a certain amount of hybridization between Ti *d* and O *p* charge causes a fraction of Ti *d* states to be occupied. This feature can be observed in Fig. 1: both e_g and t_{2g} states are hybridized with the O *p*-type manifold. By integrating the partial DOS, we can calculate orbital occupation numbers and static ionic

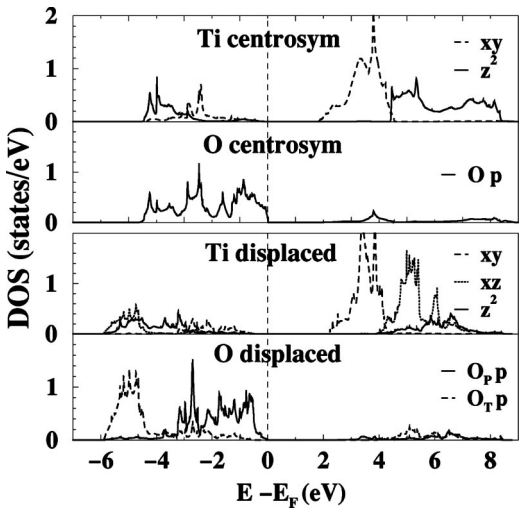

FIG. 1. Orbital-resolved density of Ti *d* and O *p* states in cubic $BaTiO_3$. The upper panel refers to the structure with atoms placed in the centrosymmetric positions, the lower panel to the structure with Ti and O atoms ferroelectrically displaced along [001] (see text).

charges. The occupation numbers of e_g and t_{2g} orbitals are 1.16 and 1.15 electrons, respectively, and the resulting ionic configuration is $Ba^{1.98+}Ti^{1.71+}O_3{}^{1.24-}$.

Previous works[2,8,9] have pointed out that this *p-d* hybridization drives the ferroelectric instability in $BaTiO_3$. To verify the sensitivity of the hybridization to atomic displacement we recalculate the orbital-resolved DOS of $BaTiO_3$, again within the cubic cell, with Ti and O atoms displaced along [001] in the fashion of a ferroelectric tetragonal distortion[30] (Fig. 1, lower panel). To emphasize the distortion effect, the displacement amplitudes have been taken to be twice as large as those of the ferroelectric tetragonal structure (i.e., $\sim 2\%$ of the theoretical lattice constant, $a_0 = 3.93$ Å).

The changes of DOS upon distortion are striking. The breaking of cubic symmetry splits the t_{2g} orbitals into one singlet (d_{xy}) and one doublet (d_{xz} and d_{yz}), and the e_g orbitals into two singlets. Among the Ti *d* orbitals d_{xy} is the least affected by the distortion since it lies on the plane orthogonal to the distortion and, moreover, is not oriented towards the ligands. Therefore it is quite insensitive to hybridization changes. In contrast, d_{z^2}, d_{xz}, and d_{yz} show remarkable changes. Furthermore, we see a large splitting between the *p* states of the oxygens in plane with Ti (O_P) and *p* states of the oxygens on top of Ti (O_T). The O_T *p* states become localized in a ~ 2 eV wide energy region located ~ 5 eV below the valence-band top and are strongly hybridized with the Ti *d* states. Analysis of the orbital characters reveals that two kinds of hybridizations between O_T *p* and Ti *d* states dominate in this range of energies: a $pd\sigma$ hybridization, mixing p_z and d_{z^2} orbitals, and a $pd\pi$ hybridization involving p_x, p_y, d_{xz}, and d_{yz}.

After the distortion, the total occupation of d_{z^2} increases from $\sim 0.6 to \sim 0.8$ electrons and that of d_{xz} (and d_{yz}) from ~ 0.4 to ~ 0.5, at the expense of the d_{xy} and O_T *p* occupations. These values suggest that **P** may be induced by inter-

TABLE I. Born effective charges Z^* and dielectric constant ϵ^∞ of ABO_3 perovskites: cubic, nonmagnetic $BaTiO_3$ and cubic antiferromagnetic $CaMnO_3$. Z^* is the component along the c axis (i.e., Z^*_{zz}); O_T and O_P label oxygens on-top and in-plane with Ti (or Mn), respectively.

	Z^*_A	Z^*_B	$Z^*_{O_T}$	$Z^*_{O_P}$	ϵ^∞
$BaTiO_3$	2.77	6.89	−5.38	−2.10	6.66
$CaMnO_3$	2.55	6.99	−5.47	−2.14	11.25

atomic charge transfer. In addition, the energy localization of the O_T p_z states is consistent with an on-site charge polarization. Eventually, both these mechanisms contribute to the polarization process.

The calculated BEC and the cubic dielectric constant are shown in Table I. Our results are in good agreement with other first-principles calculations.[8] For Ti and O_T the BEC's are highly anomalous, with magnitudes much greater than the nominal values +4 and −2, respectively.

In summary, our results are completely consistent with the picture of $BaTiO_3$ resulting from previous works: a strong change of p-d hybridization accompanies the ferroelectric displacements. But it also suggests an aspect that has not been emphasized so far: not the whole O p and Ti d manifold, but only those states derived from orbitals oriented in the direction of the ferroelectric displacement really contribute to the hybridization changes and have an active role in the polarization mechanism. In other words, an orbital is more sensitive to structural distortions if it is oriented along the displacement. In the case of $BaTiO_3$ the charge is sensitive to displacements along every direction, since all the Ti d orbitals are (formally) empty. This is consistent with the observation that in $BaTiO_3$ three ferroelectric phases polarized along the three high-symmetry directions are more stable than the cubic phase. But we will show that for other compounds with nonzero d occupations (e.g., $YMnO_3$) the orientation of the polarization is constrained to a specific direction by the details of the orbital occupations.

B. $CaMnO_3$

As a next step in understanding the interplay between electric and magnetic ordering, we now investigate a nonferroelectric magnetic perovskite whose valence environment is close to that of $BaTiO_3$. For this purpose, $CaMnO_3$ is the optimal subject: it has the same ionic configuration as $BaTiO_3$ ($Ca^{2+}Mn^{4+}O_3{}^{2-}$) and is also insulating. Furthermore, there is a large amount of experimental and theoretical information available for $CaMnO_3$.[6] The nominal configuration favors a cubic antiferromagnetic (AFM) insulating ground state, since Mn^{4+} has three d electrons placed in the triply degenerate spin-split $t^{\uparrow}_{2g}$ bands.[31] This fully occupied, spherically symmetric shell behaves as a core charge, strongly localized in space and very stable in energy.

The magnetic ordering is G-type AFM; i.e., the magnetic moment on each Mn is antiparallel to those of the six nearest-neighbor Mn ions. The unit cell has fcc symmetry and ten atoms. Since the two Mn ions in the unit cell are connected by AFM symmetry, their magnetic moments are exactly equal in magnitude and opposite in sign, while magnetic moments on O and Ca are constrained to be zero by symmetry. Our lattice constant calculated for the G-type AFM phase equals the experimental value $a_0 = 7.05$ Å.[32]

To reinforce our intuition that the Mn^{4+} ion with three electrons in the $t^{\uparrow}_{2g}$ shell is strongly resistant to off-center displacement, we calculated the energy difference between the observed centrosymmetric structure and a hypothetical tetragonal ferroelectric phase, where the atomic displacements for the latter were taken equal to those of the corresponding phase of $BaTiO_3$. The centrosymmetric configuration is lower in energy by 0.16 eV per formula unit (a huge value, compared to the small differences obtained between the various phases in $BaTiO_3$). For a volume increase of ~2%, this energy difference decreases to 0.12 eV per formula unit. Thus, as in the case of $BaTiO_3$, the competition between structural phases is affected by the volume, but in $CaMnO_3$ the equilibrium structure is so far from being ferroelectric that volume effects are not an issue.

In Figs. 2 and 3 we report our DOS calculations for the AFM-ordered phase. The technical features are the same as those already discussed for $BaTiO_3$: the DOS is orbital resolved and is calculated twice, with atoms in cubic symmetry and with Mn and O displaced along [001] (the distortion amplitude is the same as that used for $BaTiO_3$). Due to AFM symmetry, the DOS of the two Mn are equal by exchange of up and down components; thus, we show just one of them.

From the Mn DOS in the undistorted cubic structure (Fig. 2, upper panel) we see that the t_{2g} bands are more localized in energy than the e_g. The on-site exchange splitting produces a ~ 2 eV gap between filled $t^{\uparrow}_{2g}$ and empty $t^{\downarrow}_{2g}$ states. The calculated fundamental gap is ~0.4 eV. The top of the valence band has relevant contributions from both O p and Mn t_{2g} states, whereas the conduction-band bottom is mainly Mn e_g in character. As in the case of $BaTiO_3$, we see that the nominal ionic configuration is not reflected by the calculations, with a notable amount of e_g states indeed being occupied. Also, the spin polarization due to t_{2g} states is reduced by the presence of a non-negligible amount of $t^{\downarrow}_{2g}$ charge. As a result, the calculated occupation numbers are 2.94 and 0.75 for $t^{\uparrow}_{2g}$ and $t^{\downarrow}_{2g}$ orbitals, and 0.90 and 0.68 for $e^{\uparrow}_g$ and $e^{\downarrow}_g$ orbitals, respectively. The resulting Mn magnetic moment is $2.41\mu_B$, due almost entirely to the polarization of the t_{2g} states. The total Mn d charge (5.27 electrons) is far larger than the nominal charge, and the resulting ionic configuration $Ca^{1.93+}Mn^{1.73+}O_3{}^{1.22-}$ is very close to that calculated for $BaTiO_3$.

But the similarity of $CaMnO_3$ and $BaTiO_3$ is not maintained in the DOS of the distorted structure: in $CaMnO_3$, the Mn and O DOS are almost insensitive to the distortion. The tetragonal field splitting of the t_{2g} manifold into d_{xy} and the doublet d_{xz} and d_{yz} is barely distinguishable. Likewise, the splittings of d_{z^2} and $d_{x^2-y^2}$ states (not shown in the figure) and of O_T p and O_P p states are very small. The charge transfer induced by the distortion is negligible (the e_g charge increases by 0.04 electrons, at the expense of the O_T p charge), and the only visible effect on the occupation num-

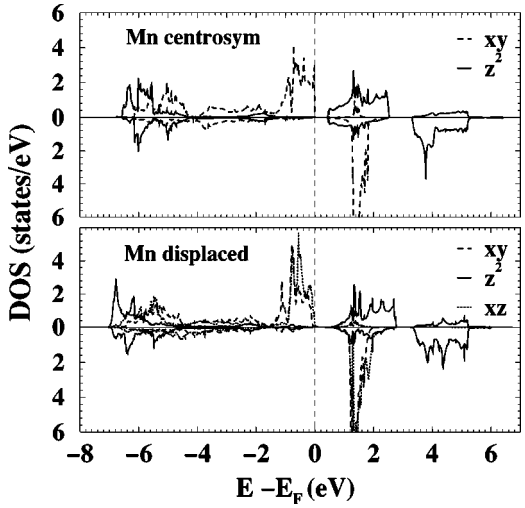

FIG. 2. Orbital-resolved DOS of a single spin-polarized Mn in AFM *G*-type $CaMnO_3$. The upper panel is for the structure with atoms placed in the centrosymmetric configuration, the lower panel for the structure with Mn and O displaced according to the ferroelectric [001] phase of $BaTiO_3$. The displacement splits the t_{2g} orbitals into one singlet d_{xy} and one doublet (d_{xz} and d_{yz}), and the e_g orbitals into two singlets.

bers is the rise of a magnetic moment on O_T as a result of the symmetry breaking. Thus, although significant *p-d* hybridization is present in the cubic ground state (revealed by the big difference of nominal and calculated *static* charges), this hybridization does not cause the occurrence of charge transfer to accompany the atomic displacements. The lack of DOS rearrangement upon ferroelectric displacements in $CaMnO_3$ is an important indication of the close relation between hybridization changes and **P**, and confirms the idea that a *change* of charge hybridization on distortion is a necessary condition for the presence of ferroelectricity.

Although BEC, static charge transfer, and hybridization changes are independent quantities for periodic systems,

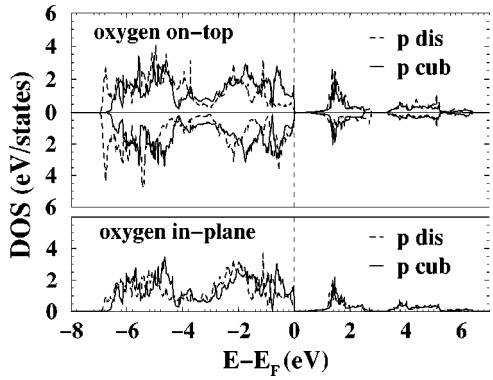

FIG. 3. Orbital-resolved DOS of a single O in AFM G-type $CaMnO_3$. Upper panel refers to O_T, i.e., the oxygen placed on top of Mn, lower panel to O_P, that is, O in-plane with Mn. Each DOS is calculated for the structure with atoms in cubic positions (cub) and for atoms displaced according to the ferroelectric [001] phase of $BaTiO_3$ (dis). Within cubic symmetry, O_T and O_P are equivalent and nonmagnetic. After the tetragonal displacement O_T becomes slightly magnetic, whereas O_P is still nonmagnetic by symmetry.

there is a common misconception that they are related. If this were true, we would expect the BEC for $CaMnO_3$ to be close to the static charges. Instead, our calculations in Table I clearly show that the BEC in $CaMnO_3$ are as anomalous as those in $BaTiO_3$. The importance of this result, we believe, deserves to be emphasized, since it shows that a highly anomalous BEC can occur even without strong hybridization changes and even in materials far from being ferroelectric. This result also raises some general questions: In which cases are the BEC highly anomalous? If the BEC anomaly is a driving force towards ferroelectricity and if $BaTiO_3$ and $CaMnO_3$ have rather similar BEC's, how can we explain their different ferroelectric properties?

The origin of the anomaly must be related to the strong *p-d* hybridization presents in $CaMnO_3$, as well as in most other perovskite oxides. The charge current flowing (i.e., percolating) through the bonds upon atomic displacement is suppressed in the limit of purely ionic interactions; thus, the BEC anomaly may be regarded as a sensitive measure of bond covalency. This argument is not in contradiction with the results for MnO,[33,34] where only a small anomaly (2.5 for the BEC of Mn) has been found, since in MnO the hybridization involves both filled O *p* and Mn *d* e_g states; thus, no net charge current can flow through the bonds [the same can be argued for ZnO (Ref. 13)].

The existence of ferroelectricity in $BaTiO_3$, and its absence in $CaMnO_3$, can be understood from two standpoints. The nonanalytical dipole-dipole term present in the dynamical matrix [responsible for the longitudinal and transverse optical phonon mode splitting at Γ (Refs. 11,35, and 36)] is

$$D^{i,j}_{\alpha\beta}=\frac{4\pi\left(\sum_{\gamma} Z^{*}_{j,\alpha\gamma}q_{\gamma}\right)\left(\sum_{\gamma} Z^{*}_{j,\beta\gamma}q_{\gamma}\right)}{\Omega\sum_{\gamma\delta} q_{\gamma}\epsilon^{\infty}_{\gamma\delta}q_{\delta}}. \qquad (6)$$

This expression shows that highly anomalous BEC should favor ferroelectricity. On the other hand, this quantity also depends on the optical dielectric constant. In Table I we also report the calculated optical dielectric constant (ϵ^{∞}) for $CaMnO_3$ and cubic $BaTiO_3$. In $CaMnO_3$, ϵ^{∞} is almost double that in $BaTiO_3$ and also considerably larger than that of the other ferroelectric perovskites [ranging from 5 to 8 (Ref. 27)]. This reflects the different degree of dispersion of the valence bands: $CaMnO_3$ is markedly more covalent than $BaTiO_3$. Such a large screening field present in $CaMnO_3$ must act as a depolarizing force counteracting the spontaneous polarization. This information is incorporated in the LEC: for $BaTiO_3$ we obtain $Z^{L}_{O_T}=0.81$ and $Z^{L}_{Ti}=1.03$, and for $CaMnO_3 Z^{L}_{O_T}=0.49$ and $Z^{L}_{Mn}=0.62$. Thus, the LEC brings out a marked difference in the behavior of these two compounds and, more generally, of nonferroelectric and ferroelectric perovskites.

Another fundamental distinction between $CaMnO_3$ and $BaTiO_3$ resides in the almost completely filled $t^{\uparrow}_{2g}$ shell of the former. This means that, unlike Ti *d*, Mn *d* orbitals cannot participate in any charge transfer or hybridization changes

with O p orbitals. Thus, the $t_{2g}^{\uparrow}$ shell, acting like a spherical core charge, always favors the centrosymmetric configuration. Since the contribution to the cohesive energy furnished by the t_{2g} orbitals is dominant with respect to that of the e_g orbitals, the presence of a filled $t_{2g}^{\uparrow}$ shell represents a major force acting against any off-center distortion. Experimentally, the absence of off-center distortion in perovskites with t_{2g}^{3} transition-metal ions (such as Mn^{4+} or Cr^{3+}) is well established.

From our analysis of $CaMnO_3$, we cannot directly relate the absence of ferroelectric distortions to the presence of the magnetic ordering, but rather to the unfavorable chemical environment due to the specific distribution of the orbital occupations. What makes the coexistence of ferroelectricity and magnetism unlikely in magnetic materials seems to be both the inability of transition metal ions with large d occupations to accept a transfer of charge from neighboring oxygens and also the strong resistance of filled d shells with spherical symmetry to move off center. However, this argument does not rule out the possibility that, in some chemical environments, the conditions of coexistence may be realized. This would require a transition-metal cation with strongly directional distribution of the d orbital occupations, in such a way that some of these orbitals along a specific direction would be unoccupied (and thus available for changes of hybridization with oxygens). In the next section we show that this is not just a theoretical hypothesis, but an occurrence verified at least in one series of compounds, i.e., the hexagonal manganese perovskites, known to be both magnetic and ferroelectric.

C. $YMnO_3$

The family of manganese perovskites crystallizes in two structural phases. The most common is the cubic or orthorhombic, found in $CaMnO_3$, $LaMnO_3$, and the manganites of the larger rare earths, from $CeMnO_3$ to $DYMnO_3$. The other phase is the hexagonal $P6_3cm$,[37,38] and includes $YMnO_3$ and the rare-earth manganites ranging from $HoMnO_3$ to $LuMnO_3$. In the rare-earth perovskites the large cation is generally completely ionized and chemically inert; thus, the occurrence of the hexagonal or cubic structure is determined only by the size of the cation, which is smaller in the class of hexagonal perovskites. These hexagonal perovskites are found to be ferroelectric along the c axis (i.e., [0001]),[38,39] with a spontaneous $\mathbf{P}\sim 5.5\mu C/cm^2$, and are magnetically ordered. Among them, $YMnO_3$ is the best known experimentally and also the most feasible for our methodology since the f states (troublesome to treat within the pseudopotential method) are empty. Also, LDA+U calculations[40] of electronic and optical properties of the hexagonal $YMnO_3$ have been recently published.[41,42]

Both (0001)-oriented films[43,44] and single crystals[37,39,45] of hexagonal $YMnO_3$ have been recently grown, and ferroelectric properties and phonon modes[39,46] have been measured. $YMnO_3$ presents some technological advantage with respect to the most common ferroelectric perovskites, like low dielectric constant ($\sim$ 20 at room temperature) and nonvolatile constituent elements. But particular excitement is due to the occurrence of ferroelectric and magnetic ordering in the same compound. The coupling between these two orderings may be eventually exploited in a device where the dielectric properties can be altered by the application of a magnetic field and the magnetic properties by that of an electric field. Although the big difference between the critical temperature of magnetic and electric orderings ($T_N=80$ K and $T_c=900$ K, respectively) may suggest that no coupling is present, some evidence of coupling has actually been observed in terms of anomalies in the dielectric constant and loss tangent at the Néel temperature.[47,48] Also, analysis of the second-harmonic optical spectra[49] of the Mn^{3+} ion shows the presence of a new kind of nonlinear optical polarization depending on two order parameters. These indications justify the effort of investigating from a theoretical point of view whether magnetic and ferroelectric ordering are reciprocally affected. Since we know the basic ingredients that favor ferroelectricity and magnetism separately, it is important to see how these elements are combined in hexagonal $YMnO_3$. Note that $YMnO_3$ is also grown in the orthorhombic phase,[50] but this phase is not ferroelectric and indeed has similar characteristics to $LaMnO_3$. Evidently, although the two phases share the same Mn^{3+} ion, the different crystal field produces drastic differences in both structural and electronic properties.

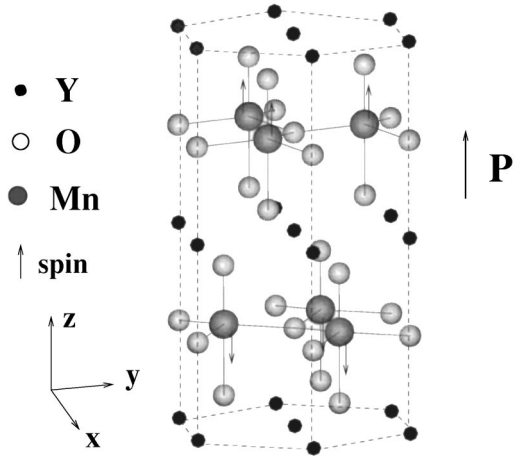

FIG. 4. Structure of the hexagonal ferroelectric $YMnO_3$. The arrows on Mn indicate the spin orientation of the A-type AFM ordering. The electric polarization **P** is directed along the c axis. A small tilting of the bipyramidal oxygen cages around Mn is neglected in figure.

In Fig. 4 a picture is shown of the ferroelectric 30-atom hexagonal unit cell in $P6_3$ cm symmetry. The Mn ions, sited on close-packed hexagonal positions, are surrounded by corner-sharing bipyramidal cages of oxygens. The stacking along the c axis consists of a $(MnO)_3$ layer, followed by three $\sqrt{3}\times\sqrt{3}$ layers containing in sequence O_3, Y_3, and O_3 (in total there are eight layers per cell). In addition the MnO_5 bipyramids are slightly rotated around the axis passing through the Mn and parallel to one of the triangular base sides. Discarding these small, barely visible tiltings, the atomic positions are those of the paraelectric ($P6_3/mmc$) phase, stable at $T>T_c$. Within the paraelectric symmetry the

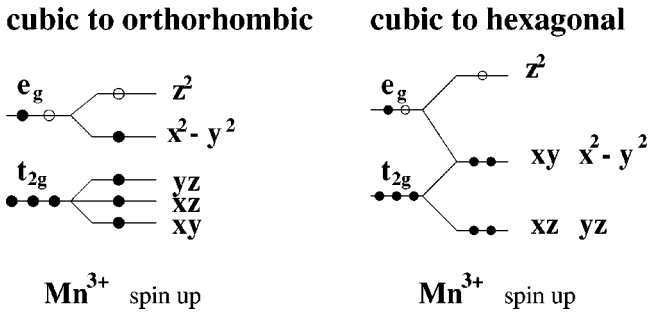

FIG. 5. Schematic orbital splitting for the majority d states of Mn^{3+} ion within orthorhombic and hexagonal crystal field.

unit cell has ten atoms distributed on eight 1×1 hexagonal layers. Since the electric polarization occurs along the c axis and the bipyramidal tilting does not alter significantly the features of this compound, the untilted structure is sufficient for the purpose of studying the changes of hybridization in the direction of the ferroelectric displacement. Thus, our calculations will be for the (ten atoms) 1×1 slab.

Regarding the magnetic ordering, hexagonal $YMnO_3$ is found to be A-type AFM (Refs. 51,52) below T_N. The spins on Mn are noncollinear and oriented in triangular fashion. For our calculation we assume the A-type AFM collinear ordering shown in Fig. 4, what we find to be slightly lower in energy than the FM ordering. However, for our purposes this is not an essential feature, since the properties that we want to investigate are determined by the local (i.e., internal to the oxygen cage) spin polarization rather than by the long-range ordering between magnetic moments.

The hexagonal paraelectric structure has three independent lattice parameters, i.e., the usual a and c parameters plus an internal u that gives the distance (in units of c) between O_3 and Y_3 layers, and is not fixed by the symmetry. By energy minimization we obtain the theoretical values $a=3.518$ Å, $c=11.29$ Å, and $u=0.084$, in very good agreement with the experimental values $a=3.539$ Å, $c=11.3(4)$ Å, and $u=0.084$. This also suggests that the oxygen tilting has only a small effect on the structural properties. The distances between Mn and O are $\Delta_{Mn\text{-}O_T}=1.875$ Å and $\Delta_{Mn\text{-}O_P}=2.03$ Å. As a point of comparison, we also calculated the structure of $YMnO_3$ within FM cubic symmetry, and found $a=3.765$ Å and $\Delta_{Mn\text{-}O}=1.878$ Å. It is notable that the volume enclosed in the bipyramidal cage of the hexagonal structure is much smaller than the octahedral volume of the cubic structure. In other words, in the hexagonal symmetry the Mn charge is enclosed in a smaller and more packed surrounding.

In Fig. 5 a scheme of the majority d-state splitting of Mn^{3+} ion due to the hexagonal crystal field is drawn, in comparison with the splitting due to the orthorhombic field. In the hexagonal field the d states are no longer split into t_{2g} and e_g states, but are ordered in two doublets and one singlet (the Cartesian axes are drawn in Fig. 4).

To determine the effect of the spin polarization we calculated the orbital-resolved DOS for the hexagonal phase with both nonmagnetic and AFM ordering. The nonmagnetic phase (Fig. 6) shows a large DOS at the Fermi energy, E_F,

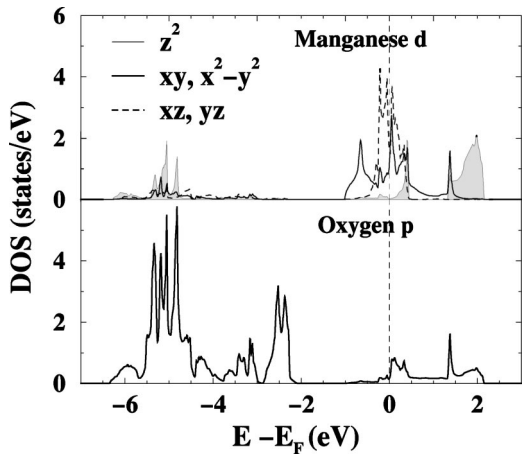

FIG. 6. Orbital-resolved density of Mn d and O_T p states for the paraelectric, nonmagnetic phase of $YMnO_3$. Since the two couples of Mn d orbitals $(d_{xy},d_{x^2-y^2})$ and (d_{xz},d_{yz}) are nearly degenerate, only one curve for each couple is shown.

mostly due to the Mn d states located in a narrow region around E_F. The degenerate d_{xy} and $d_{x^2-y^2}$ orbitals (of which only one is reported in the figure) lie on the (0001) plane and point towards O_P, thus contributing to the covalent bonding. The d_{xz} and d_{yz} orbital DOS overlap with those of d_{xy} and $d_{x^2-y^2}$, but are localized in a narrower energy region, since they do not point towards oxygens and are more localized in space. Finally, d_{z^2} is the highest in energy and the least occupied, but a certain amount of d_{z^2} charge is hybridized with the O_T p_z states located ~5 eV below E_F.

From this energy ordering of the orbitals it follows that each of the four lowest-lying d orbitals is roughly half-occupied and contributes to a large DOS at E_F. According to the Stoner exchange argument, this large DOS represents a strong driving force towards a spin-polarized stable phase. Indeed, we find that the transition from nonmagnetic to AFM ordering results in a large energy gain ($\sim$ 1.6 eV per formula unit).

In Fig. 7 we report the orbital-resolved DOS of individual spin-polarized Mn and O atoms. As in the case of $CaMnO_3$, the AFM symmetry enforces the DOS of the two Mn atoms within the unit cell to be equal under exchange of up and down components. The energies of the Mn d manifold are spin split by $\sim$ 2.5 eV, and the two doublets of Mn d states become almost completely spin polarized. Their total up and down charges are 3.93 and 0.47 electrons, respectively, while the occupation numbers of $d_{z^2}^{\uparrow}$ and $d_{z^2}^{\downarrow}$ orbitals are 0.53 and 0.30 electrons. The resulting magnetic moment on Mn $(3.7\mu_B)$ is consistent with the high-spin state $S=2$, although smaller than $4\mu_B$ due to the partial hybridization of d_{z^2} with O_T p_z states, and of d_{xy} and $d_{x^2-y^2}$ with O_P p_x and p_y states. A non-negligible magnetic moment $M=0.15\mu_B$ is also present on O_P, driven by double exchange with the d_{xy} and $d_{x^2-y^2}$ orbitals, whereas the magnetization of O_T is almost vanishing, due to the AFM symmetry (for $u=0$ it would be exactly zero). However, the spin splitting is not large enough to open a gap within the LSDA. Indeed there is a tiny DOS

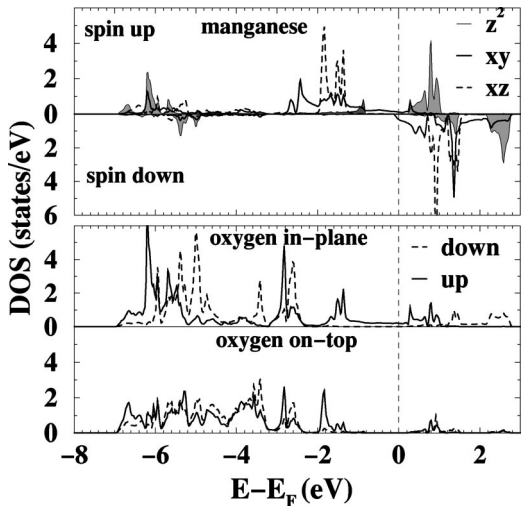

FIG. 7. Orbital-resolved DOS of single Mn (top panel), O_P (middle), and O_T (bottom) in the paraelectric AFM phase of $YMnO_3$. Due to the exact AFM symmetry, each of the atoms reported in the figure has a corresponding atom in the cell with antialigned spin, i.e., with up and down components of DOS exchanged.

at E_F, to which d_{xy} and $d_{x^2-y^2}$ orbitals from Mn and p_x and p_y orbitals from O_P contribute. Notice that these orbitals all lie in the hexagonal plane.

The mainly planar distribution of the charge density is also evident from the band energies shown in Fig. 8. The bands are calculated within the $(k_x,k_y,0)$ plane of the Brillouin zone (left panel), and along $\mathbf{k}=[0,0,k_z]$ (right panel). (Note that up and down bands are degenerate in the AFM phase.) Only one band crosses E_F at $k_z=0$, and its orbital character is a mix of $d^{\uparrow}_{xy}$ and $d^{\uparrow}_{x^2-y^2}$ states from Mn and $p^{\uparrow}_x$ and $p^{\uparrow}_y$ states from O_P. The band energies are extremely flat along [0001], as is typical for strongly layered compounds.

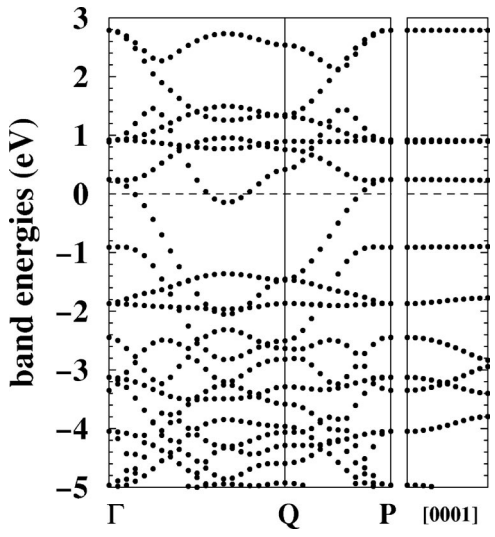

FIG. 8. Band energies of the paraelectric AFM $YMnO_3$. The left panel shows results for the $\mathbf{K}_z=0$ hexagonal plane [i.e., $Q=\pi/a(0,2/3^{1/2},0), P=\pi/a(1,1/3^{1/2},0)=\Gamma$]; the right panel shows the band energies calculated along $[0,0,k_z]$.

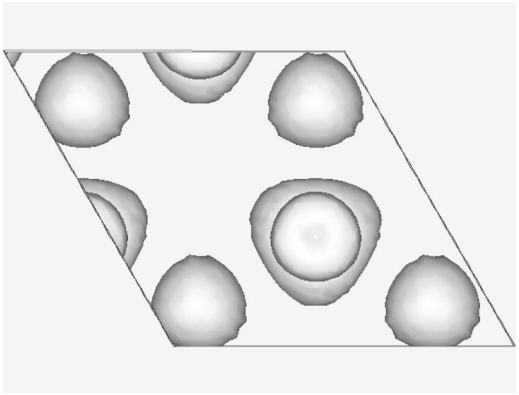

FIG. 9. Top view of the charge isosurface of paraelectric AFM $YMnO_3$. Only the charge of states lying within a small energy interval below E_F has been considered. The triangularly-shaped charges are centered on Mn and represent planar *d* orbitals. On top of each Mn, the charge of O_T *p* states appears to be spherical, whereas a slight triangular shape is visible in the charge of the three in-plane oxygens surrounding Mn.

Since the experimental findings suggest that this system is an insulator, the presence of some DOS at E_F must be attributed to the usual inadequacy of the LSDA to describe the magnetic perovskites as insulators. The source of error favoring a metallic ground state is primarily the insufficient spin splitting of the Mn *d*-state manifold and also a slight overestimation of the hybridization between d_{xy} and $d_{x^2-y^2}$ orbitals and O_P p_x and p_y orbitals. (Indeed in Ref. 41 it is shown that the introduction of an Hubbard correction $U=8$ eV onto the Mn *d* bands opens a gap $\sim$ 1.5 eV and decreases the in-plane O *p*–Mn *d* hybridization.) In terms of calculating the ferroelectric properties, the metallic character found in the LSDA calculations is obviously annoying, since the metallicity destroys the possibility of sustaining a spontaneous electric polarization. For this reason we cannot report here a study of structural stability of the ferroelectric phase. However, we emphasize that, even if the energy gap is not properly described, the LSDA is generally accurate in calculating magnetic moments, orbital occupation numbers, and atomic charges of magnetic perovskites so that our arguments based on these quantities are still valid.

A useful perspective of the charge distribution is also given by the isosurfaces of the charge and spin density. In Fig. 9 the top view onto the (0001) layer of a charge isosurface is shown. To better distinguish the orbital shapes, the isosurfaces are not extracted from the total charge but only from the charge of the states whose energy is within ~ 2 eV from E_F. A triangular shape of charge around Mn is visible, with the O_T charge superimposed, surrounded by the almost spherical charge of the three O_P neighbors. Since the Mn DOS is completely spin polarized in the region just below E_F, the charge isosurface surrounding Mn is also a magnetization isosurface. In Fig. 10 a three-dimensional view of a magnetization isosurface (due to states within ~ 2 eV from E_F) is shown. Light and dark sections distinguish spin-up and spin-down densities (i.e., isosurfaces with opposite signs). We can clearly see the oxygen cage surrounding Mn, whereas no charge is visible for Y. The magnetization is dis-

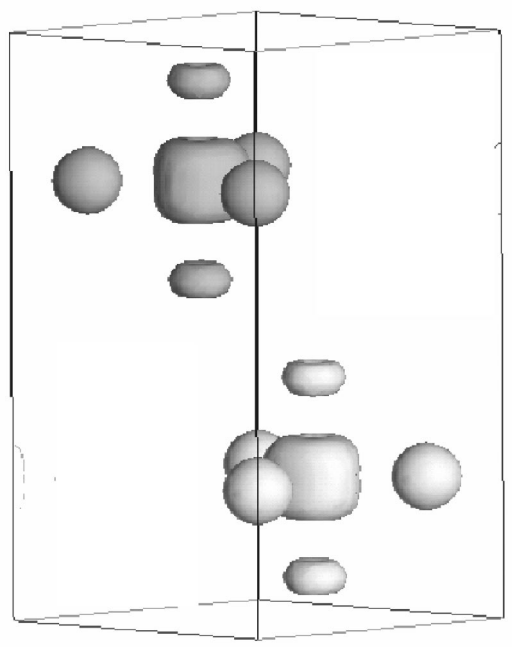

FIG. 10. Three-dimensional view of the magnetization isosurfaces. Light and dark surfaces represent magnetizations with the same magnitude but opposite sign, i.e., up and down spin densities. Only the charge of states lying within a small energy interval below E_F has been considered.

tributed more in plane than orthogonally, and a strong asymmetry between O_P and O_T is also visible. The former has a rather spherical charge distribution, whereas the latter shows a prevalence of p_x and p_y orbitals.

Analogous to our calculations for $BaTiO_3$ and $CaMnO_3$, we now look at the sensitivity of the charge distribution to atomic displacements by moving Mn and O against each other along direction [0001]. To make a consistent comparison with the results found for the other perovskites, the amplitude of the atomic displacements are taken equal to those of the other cases. The corresponding DOS is shown in Fig. 11. For clarity, only d_{xz} and d_{z^2} (i.e., the orbitals not lying in the hexagonal plane) are shown, since they are the most affected by the displacements. For these orbitals the change of DOS upon distortion is very evident and is similar to that observed in $BaTiO_3$. The d states are shifted downward in energy by ~ 2 eV and strongly hybridized with the O_T p states that are localized in a ~ 1-eV-wide energy region. The dominant hybridizations are the same as those found in $BaTiO_3$: the displacements enhance the $pd\sigma$ hybridization involving d_{z^2} and O_T p_z orbitals and the $pd\pi$ hybridization between d_{xz}, d_{yz}, and O_T p_x and p_y orbitals.

We do not find substantial changes in the occupation numbers of d and p orbitals upon distortion. This might suggest that there is not an interatomic charge transfer, but this conclusion may be debated. Indeed, the O_T DOS in the centrosymmetric structure is quite broadened into a large (~ 6 eV) energy range, indicating that the corresponding charge density is largely scattered into the interstitial regions. Upon distortion, instead, it becomes much more localized (in energy and space), and thus it can be more properly recognized as charge sited on O_T.

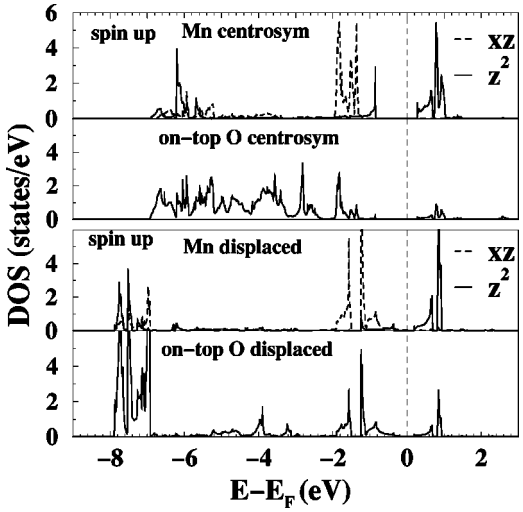

FIG. 11. Orbital-resolved DOS for single Mn and O in hexagonal AFM $YMnO_3$. The upper panel is for the paraelectric structure, the lower for the structure with Mn and O displaced along the c axis, in the fashion of a ferroelectric distortion.

From the DOS analysis, we see that the peculiar behavior of hexagonal $YMnO_3$ can be understood on the basis of orbital arrangement and crystal field splitting. Unlike the cubic phase, where the partial occupation of the e_g states causes a Jahn-Teller distortion, in the hexagonal phase four d orbitals are filled and one is (nominally) empty. Thus, the latter (d_{z^2}) can be actively involved in strong changes of hybridization with the O_T p_z orbitals, realizing the same kind of chemical behavior that drives the ferroelectricity in $BaTiO_3$.

However, in contrast to $BaTiO_3$ where all the d states are formally empty and able to contribute to hybridization changes, in hexagonal $YMnO_3$ we expect that the ferroelectric displacement will only be energetically favored along [0001]. This observation leads us to suggest a generalized criterion of *directional* "d^0-ness": in order for a chemical environment to be favorable to ferroelectric distortions, the d orbitals *in the direction of the electric polarization* must be empty.

We emphasize that this chemical environment favorable to the electric polarization along the c axis is only realized in the spin-polarized phase, and not in the nonmagnetic hexagonal phase. In other words, in hexagonal $YMnO_3$ the spin polarization not only does not prevent, but is actually necessary to enable the ferroelectricity. Also, notice that the transition from the AFM to the paramagnetic phase above $T_N = 80$ K (i.e., well below the critical temperature of the ferroelectric phase) does not invalidate our argument, since it is the local spin-polarization of Mn^{3+} that matters, independently of the actual presence (or absence) of long-range spin ordering.

At this stage of the investigation we cannot affirm that the chemical activity of Mn d_{z^2} and O_T p_z orbitals alone is sufficient to explain the spontaneous polarization.[53] To confirm this, a study of the properties of the ferroelectric phase (which is inaccessible in the LSDA) will be necessary.[54] It will be particularly important to evaluate the BEC. We are not aware of any existing experimental or theoretical deter-

mination. However, we might expect anomalous values on Mn and O_T in the direction of the proposed ferroelectric distortion.

IV. CONCLUSIONS

In this paper we have investigated three perovskite oxides in order to understand under which conditions the rare coexistence of magnetic and ferroelectric orderings can take place.

The comparison of $BaTiO_3$ and $CaMnO_3$ showed relevant differences in DOS and sensitivity of orbital hybridization to ferroelectric displacements. In $BaTiO_3$ a ferroelectric distortion causes a strong enhancement of $pd\sigma$ and $pd\pi$ hybridizations involving those Ti *d* orbitals having a component along the direction of the polarization axis. In $CaMnO_3$, however, the DOS and orbital occupation numbers are mostly unaffected by the same displacements, in spite of the fact that the *p*-*d* hybridization is stronger in $CaMnO_3$ than in $BaTiO_3$. Thus, our results indicate that ferroelectric distortions are likely driven by strong *changes* of hybridization upon atomic displacement, whereas a strong hybridization is, in itself, not a sufficient condition to expect ferroelectricity.

On the other hand, perhaps unexpectedly, the BEC's in $CaMnO_3$ are found to be as anomalous as those in $BaTiO_3$. To our knowledge, this is the first report of a highly anomalous BEC for a magnetic perovskite. This result stresses that effective charges and static charges provide quite independent information, and indicates that the BEC anomaly may be a common feature of the whole perovskite family, rather than just of the ferroelectric compounds.

In addition, the optical dielectric constant is much larger in $CaMnO_3$ than in $BaTiO_3$. A larger electron screening gives a smaller tendency towards spontaneous electric polarizability, and also affects the splitting of longitudinal and transverse phonon modes at Γ. Since the longitudinal charges contain the screening information, they may be better indicators of ferroelectric instability than the BEC.

Our comparative study of $BaTiO_3$ and $CaMnO_3$ suggests a simple reason for the lack of coexistence of magnetic and electric polarization: the cation *d* orbitals need to be empty in order to be available for hybridization changes with O *p* states. At first sight this requirement rules out the simultaneous presence of magnetism and ferroelectricity. A counterexample to this argument is furnished by the hexagonal $YMnO_3$, which is ferroelectric and antiferromagnetic. Our investigation gives an argument to solve this apparent contradiction and suggests a generalization of the previous picture: in the hexagonal perovskites the crystal field of the spin-polarized phase causes an ordering that leaves the high energy d_{z^2} orbital mostly unoccupied and available for hybridization changes with p_z orbital of the on-top oxygen. Thus, a single, empty, *d* orbital in a favorable energy range for hybridization with oxygen may be sufficient to induce a strong tendency towards ferroelectric distortion polarized in the direction of this orbital (directional "d^0-ness").

Note that, despite the presence of the same Mn^{3+} ion, the physics of orthorhombic and hexagonal $YMnO_3$ is very different, due to the different crystal field. In the former structure the Mn^{3+} ion has partially occupied e_g states. This creates an instability relieved by Jahn-Teller distortion and the ordering of Mn orbitals on the (001) plane. Both Jahn-Teller and orbital ordering are unlikely to allow any ferroelectric distortion, since they favor structural configurations that keep Mn and O aligned on the same plane.

Finally, the role of the filled *d* orbitals can be very important. It is intuitive that in $CaMnO_3$ the filled, corelike Mn *d* $t_{2g}^{\uparrow}$ orbitals furnish a robust counteraction to off-center distortions, since they do not participate in hybridization changes with oxygens. In other words, they cannot be destabilized since their electron charge tends to remain centrosymmetrically distributed upon distortion. In contrast, in hexagonal $YMnO_3$, the opposition of the four filled *d* orbitals (mainly laying in the *x*-*y* plane) to ferroelectric distortions along the *c* axis is arguably weaker, since $YMnO_3$ is less stiff along the *c* axis than in the *x*-*y* plane.

Of course, much work still needs to be done in order to reach a complete understanding of ferroelectric and magnetic coexistence. A fundamental aspect is related to a methodological advancement. It is indeed necessary to set feasible schemes capable of correcting the major deficiencies of the LSDA and accessing in a reliable way the full range of both ferroelectric properties (including spontaneous polarization, BEC, and piezoelectric tensor) and magnetic properties (including noncollinearity and spin-orbit interaction).

ACKNOWLEDGMENTS

We acknowledge financial support from the National Science Foundation, Division of Materials Research, under Grant No. DMR 9973076. Also, this work made use of MRL Central Facilities supported by the National Science Foundation under Award No. DMR00-80034. Most of the calculations have been carried out on the IBM SP2 machine of the MHPCC Supercomputing Center in Maui, HI.

[1] R.E. Cohen and H. Krakauer, Phys. Rev. B **42**, 6416 (1990).

[2] R.E. Cohen, Nature (London) **358**, 136 (1992).

[3] S. Baroni, P. Giannozzi, and A. Testa, Phys. Rev. Lett. **58**, 1861 (1987); X. Gonze, D.C. Allan, and M.P. Teter, *ibid.* **68**, 3603 (1992); X. Gonze, Phys. Rev. B **55**, 10 337 (1997); X. Gonze and Ch. Lee, *ibid.* **55**, 10 355 (1997).

[4] R. Resta, Ferroelectrics **136**, 51 (1992); Europhys. Lett. **22**, 133 (1993); Rev. Mod. Phys. **66**, 899 (1994).

[5] R.D. King-Smith and D. Vanderbilt, Phys. Rev. B **47**, 1651 (1993); D. Vanderbilt and R.D. King-Smith, *ibid.* **48**, 4442 (1993).

[6] An extremely vast literature about $CaMnO_3$ has been produced in the last five years. For a recent review see *Physics of Manganites*, edited by T. A. Kaplan and S. D. Mahanti (Kluwer/Plenum,

New York, 1999).
[7] N.A. Hill, J. Phys. Chem. B **104**, 6694 (2000).
[8] Ph. Ghosez, J.-P. Michenaud, and X. Gonze, Phys. Rev. B **58**, 6224 (1998).
[9] R. Resta, M. Posternak, and A. Baldereschi, Phys. Rev. Lett. **70**, 1010 (1993).
[10] M. Posternak, R. Resta, and A. Baldereschi, Phys. Rev. B **50**, 8911 (1994).
[11] W. Zhong, R.D. King-Smith, and D. Vanderbilt, Phys. Rev. Lett. **72**, 3618 (1994).
[12] Ph. Ghosez, X. Gonze, and J.-P. Michenaud, Ferroelectrics **153**, 91 (1994).
[13] For example, in ZnO the strong *p-d* hybridization is responsible for the large piezoelectricity, but does not cause either the BEC anomaly or ferroelectricity: N.A. Hill and U. Waghmare, Phys. Rev. B **62**, 8802 (2000).
[14] The BEC's are larger than the formal charges (although perhaps not large enough to be described as ''anomalous'') not only in ferroelectric perovskites, but also in some nonferroelectric rock-salt oxides (Ref. 15) (e.g., CaO, SrO, BaO) and rutiles (Ref. 16) (TiO_2).
[15] M. Posternak, A. Baldereschi, S. Massidda, and R. Resta, Bull. Am. Phys. Soc. **41**, 493 (1996); M. Posternak, A. Baldereschi, H. Krakauer, and R. Resta, Phys. Rev. B **55**, R15 983 (1997).
[16] Ch. Lee and X. Gonze, Phys. Rev. B **49**, 14 730 (1994); Ch. Lee, Ph. Ghosez, and X. Gonze, *ibid.* **50**, 13 379 (1994).
[17] We use a verison of PWSCF code originally implemented in SISSA, Trieste, and generalized by one of the authors to allow for spin polarization.
[18] D.M. Ceperley and B.J. Alder, Phys. Rev. Lett. **45**, 566 (1980); J.P. Perdew and A. Zunger, Phys. Rev. B **23**, 5048 (1981).
[19] D. Vanderbilt, Phys. Rev. B **32**, 8412 (1985).
[20] H.J. Monkhorst and J.D. Pack, Phys. Rev. B **13**, 5188 (1976).
[21] Ph. Ghosez, X. Gonze, Ph. Lambin, and J.-P. Michenaud, Phys. Rev. B **51**, 6765 (1995); L.L. Boyer, H.T. Strokes, and M.J. Mehl, Ferroelectrics **194**, 173 (1996).
[22] R. Resta and K. Kunc, Phys. Rev. B **34**, 7146 (1986).
[23] F. Bernardini, V. Fiorentini, and D. Vanderbilt, Phys. Rev. Lett. **79**, 3958 (1997).
[24] M. E. Lines and A. M. Glass, *Principles and Applications of Ferroelectric and Related Materials* (Clarendon Press, Oxford, 1977).
[25] M. Yamaguchi, K. Inoue, T. Yagi, and Y. Akisage, Phys. Rev. Lett. **74**, 2126 (1995).
[26] Ph. Ghosez, X. Gonze, and J.-P. Michenaud, Europhys. Lett. **33**, 713 (1996).
[27] Ph. Ghosez, E. Cockayne, U.V. Waghmare, and K.M. Rabe, Phys. Rev. B **60**, 836 (1999).
[28] W. Zhong, D. Vanderbilt, and K.M. Rabe, Phys. Rev. Lett. **73**, 1861 (1994); Phys. Rev. B **52**, 6301 (1995).
[29] J. Padilla, W. Zhong, and D. Vanderbilt, Phys. Rev. B **53**, R5969 (1996).
[30] In the tetragonal distortion Ba are kept fixed, while O and Ti are moved against each other. The displacement ratios are $\Delta R_{O_T}/\Delta R_{Ti} \sim -2$ and $\Delta R_{O_p}/\Delta R_{Ti} \sim -1$.
[31] For a nice overview of the main features of magnetic ordering in manganise perovskites see D.I. Khomskii and G.A. Sawatzky, Solid State Commun. **102**, 87 (1997).
[32] Although this perfect agreement may be fortuitous, it has been shown that LSD calculations accurately describe the properties of $CaMnO_3$ (for example, the observed *G*-type AFM ordering is correctly found to be the lowest in energy).
[33] S. Massidda, A. Continenza, M. Posternak, and A. Baldereschi, Phys. Rev. Lett. **74**, 2323 (1995); Phys. Rev. B **55**, 13 494 (1997); S. Massidda, M. Posternak, A. Baldereschi, and R. Resta, Phys. Rev. Lett. **82**, 430 (1999).
[34] R. Resta, J. Phys. Chem. Solids **61**, 153 (2000).
[35] P. Giannozzi, S. de Gironcoli, P. Pavone, and S. Baroni, Phys. Rev. B **43**, 7231 (1991).
[36] X. Gonze, J.-C. Charlier, D.C. Allan, and M.P. Teter, Phys. Rev. B **50**, 13 035 (1994).
[37] H.L. Yakel, W.C. Koehler, E.F. Bertaut, and E.F. Forrat, Acta Crystallogr. **16**, 957 (1963).
[38] N. Fujimura, T. Ishida, T. Yoshimura, and T. Ito, Appl. Phys. Lett. **69**, 1011 (1996).
[39] S.H. Kim, S.H. Lee, T.H. Kim, T. Zyung, Y.H. Jeong, and M.S. Jang, Cryst. Res. Technol. **35**, 19 (2000).
[40] V.I. Anisimov, J. Zaanen, and O.K. Andersen, Phys. Rev. B **44**, 943 (1991).
[41] J.E. Medvedeva, V.I. Anisimov, M.A. Korotin, O.N. Mryasov, and A.J. Freeman, J. Phys.: Condens. Matter **12**, 4947 (2000).
[42] M. Qian, J. Dong, and D.Y. Xing, Phys. Rev. B **63**, 155101 (2001).
[43] T. Yoshimura, N. Fujimura, and T. Ito, Appl. Phys. Lett. **73**, 414 (1998).
[44] W.-C. Yi, J.-S. Choe, C.-R. Moon, S.-I Kwun, and J.-G. Yoon, Appl. Phys. Lett. **73**, 903 (1998).
[45] B.B. van Aken, A. Meetsma, and T.T.M. Palstra, Acta Crystallogr. **57**, 230 (2001).
[46] M.N. Iliev, H.-G. Lee, V.N. Popov, M.V. Abrashev, A. Hamed, R.L. Meng, and C.W. Chu, Phys. Rev. B **56**, 2488 (1997).
[47] Z.J. Huang, Y. Cao, Y.Y. Sun, Y.Y. Xue, and C.W. Chu, Phys. Rev. B **56**, 2623 (1997).
[48] T. Katsufuji, S. Mori, M. Masaki, Y. Moritomo, N. Yamamoto, and H. Takagi, Phys. Rev. B **64**, 104419 (2001).
[49] D. Fröhlich, St. Leute, V.V. Pavlov, and R.V. Pisarev, Phys. Rev. Lett. **81**, 3239 (1998).
[50] M.N. Iliev, M.V. Abrashev, H.-G. Lee, V.N. Popov, Y.Y. Sun, C. Thomsen, R.L. Meng, and C.W. Chu, Phys. Rev. B **57**, 2872 (1998).
[51] W. Sikora and V.N. Syromyatnikov, J. Magn. Magn. Mater. **60**, 199 (1986).
[52] D. Fröhlich, St. Leute, V.V. Pavlov, R.V. Pisarev, and K. Kohn, J. Appl. Phys. **85**, 4762 (1999).
[53] During the review process of this work, new structural data of single-crystal $YMnO_3$ have been published (Ref. 45) which seem to challenge previous measurements (Ref. 37) and suggest that the major off-center distortion does not reside on Mn but on Y, as a consequence of oxygen rotations. Eventually, both these displacements may contribute to the ferroelectric state.
[54] We are currently implementing a method based on self-interaction corrected pseudopotentials (Ref. 55) which seems promising of improving the LSDA results. Another interesting approach recently applied to study magnetic materials is the model GW used in Ref. 33.
[55] D. Voegel, P. Krüger, and J. Pollmann, Phys. Rev. B **54**, 5495 (1996).